Soft Matter

Dynamic Article Links

Cite this: *Soft Matter*, 2012, **8**, 11704

www.rsc.org/softmatter

**PAPER**

# Controlling uni-directional wetting *via* surface chemistry and morphology†

**Levent Kubus,[ab] Hakan Erdogan,[a] Erhan Piskin[bc] and Gokhan Demirel*[ac]**

***Received 12th July 2012, Accepted 5th September 2012***
**DOI: 10.1039/c2sm26619a**

Inspiration from natural designs offers opportunities to develop novel functional materials having unique properties. An active area of research in this field is the construction of anisotropic nanostructured surfaces, which exhibit direction dependent wetting behavior. Here, we demonstrated the effects of surface chemistry and morphology on the directional wetting phenomenon. The nanofilms having directionality were fabricated at varying tilt angles ($\beta$) *via* oblique angle deposition (OAD) technique. The chemical modifications of engineered nanofilms were then carried out by using thiol molecules having different end groups (*i.e.*, $-CF_3$, $-CH_3$, and –phenyl). We found that surface morphology and chemistry are extremely important parameters in the control of directional wetting. By this way, it was possible to manipulate the movement of a water droplet on the nanostructured surfaces. Such a control would have a great impact for several technological applications involving catalysis, tissue engineering, and biosensors.

## Introduction

With millions of years of evolution, nature has learned how to use minimum resources to achieve maximal performance, and then created unique biological materials possessing hierarchical micro and nanoscale structured surface, which may exhibit excellent wettability properties.[1,2] For ages, inspirations from natural features in synthetic materials have been an interest to develop new methods and approaches.[3,4] A closer look at natural creatures reveal organized structured features at both microscopic and macroscopic scale and mainly composed of millions of aligned columns which create direction dependent properties.[5,6] Similarly, well-ordered arrays of synthetic nanostructures can be readily fabricated through templating, chemical vapor deposition, oblique angle polymerization, lithography, and self-assembly.[7–11] In particular, oblique angle deposition is a simple yet versatile technique to create anisotropic textured materials having direction-dependent properties.[12]

The directional wetting of anisotropic surfaces of interest in our work was first demonstrated by Demirel and co-workers, where the directional surfaces were fabricated by oblique angle polymerization of dichloro-[2,2]-paracyclophane.[13] Although they succeeded to demonstrate pin and release behavior of a droplet upon direction, the effects of surface chemistry and morphology of the nanofilms on the directional wetting phenomenon have largely been unexplored due to the difficulties in the post-modification and fabrication of directional polymeric nanostructures having varying end groups or tilt angles. Recently, Neuhaus *et al.* reported the influence of surface chemistry on the anisotropic wetting of structured surfaces, which were produced by hot embossing method.[14] They showed that water droplets propagate in parallel and perpendicular to the microstructures which were modified with hydrophobic polymer brushes, whereas they were strongly pinned to the hydrophilic surfaces. However, we should note that directional wetting phenomenon and anisotropic liquid spreading seems to originate from a similar basis, but they are different area of interests.

Herein, we reported the effects of surface chemistry and morphology on the engineered gold nanofilms having directional nanostructures. Our nanofilms with varying tilt angles were fabricated using oblique angle deposition technique, and modified *via* well-known thiol chemistry (Fig. 1). We demonstrated that the surface chemistry and morphology is absolutely critical in the directional wetting phenomenon.

## Experimental

The directional gold nanofilm arrays were fabricated in a physical vapor deposition system (NANOVAK HV, Ankara, Turkey) using a homemade OAD equipment. Fig. 1 shows a schematic representation of a typical deposition process. For the deposition, p-type silicon wafer and BK7 glass slides were used as a substrate. The directional nanofilms were created at different

[a]*Bio-inspired Materials Research Laboratory (BIMREL), Department of Chemistry, Gazi University, 06500, Ankara, Turkey. E-mail: nanobiotechnology@gmail.com; Fax: +90 312 2122279; Tel: +90 312 2021530*

[b]*Department of Chemical Engineering, Hacettepe University, 06532 Ankara, Turkey*

[c]*Biyomedtek: Center for Bioengineering, 06532, Ankara, Turkey*

† Electronic supplementary information (ESI) available: Cross-section and top-view SEM images of engineered nanofilms. XRD pattern for fabricated AuNRs. AFM images of deposited nanostructures at different tilt angles. Calculated retention forces of modified surfaces as a function of substrate tilt angle. A video about pin and release behavior of engineered gold nanofilms. See DOI: 10.1039/c2sm26619a

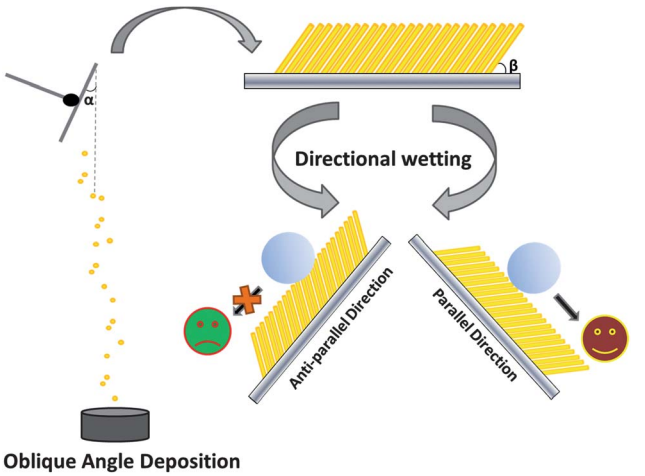


**Fig. 1** Schematic representation of OAD procedure and directional wetting phenomenon.

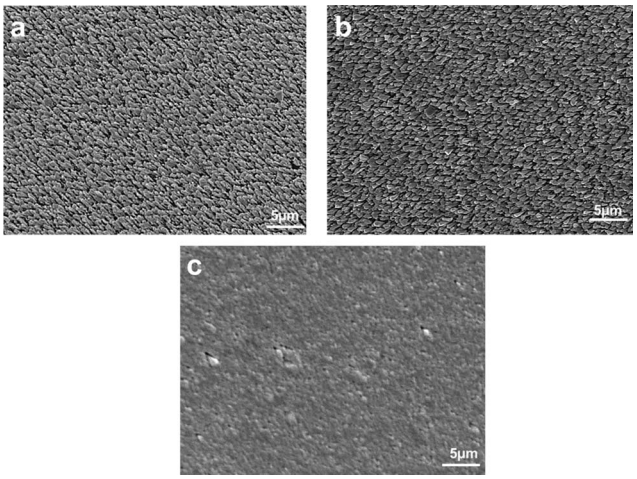


**Fig. 2** Top-view SEM images of fabricated gold nanofilms at (a) $\alpha = 5°$, (b) $\alpha = 10°$, and (c) $\alpha = 20°$.

deposition angles of $\alpha = 5°$, 10°, and 20°. For comparison, the flat gold films were also fabricated at $\alpha = 90°$. The thickness of deposited films was monitored *in situ* by a quartz crystal microbalance (QCM). During deposition, the base pressure was about $\sim 10^{-6}$ Torr, and evaporation rate was 0.1 Å $s^{-1}$. As-deposited nanofilms were then characterized by a JEOL JSM-6060 scanning electron microscope (SEM) with an acceleration voltage of 10 kV. The SEM images were then analyzed with the freeware IMAGEJ image analysis software.

To improve wetting properties, the gold nanofilms were modified using different thiol molecules having varying end groups (–$CF_3$, –$CH_3$, and –phenyl). Briefly, the nanofilms were first cleaned using a UV-ozone cleaner (Model 42, Jelight Company Inc. USA) for 15 min, and then modified in a vacuum oven at 180° for 3 h using ~500 μL of 1*H*,1*H*,2*H*,2*H*-perfluorodecanethiol for –$CF_3$, 1-dodecanthiol for –$CH_3$, and thiophenol for –phenyl end groups, respectively. The static and dynamic contact angle measurements were carried out at 25 °C in ambient air using an automatic contact angle goniometer equipped with a flash camera (DSA 100 Krüss, Germany). The contact angles were calculated by using the software of the instrument. In directional wetting, critical droplet volumes were also determined with increasing water droplet volume until the droplet slide on the tilted substrate. Note that the values reported here are the averages of at least three measurements taken at three different locations on each sample surface. Deionized water was used for all contact angle measurements.

## Results and discussion

In order to evaluate the effects of the surface morphology and chemistry on the directional wetting phenomenon, anisotropic gold nanostructures having varying tilt angles ($\beta$) were first fabricated onto the solid surfaces (*i.e.*, BK7 glass slide or silicon wafer) *via* the well-known oblique angle deposition (OAD) technique. Fig. 2 shows the top-view SEM images of the deposited gold nanostructures on the glass surfaces. The SEM images clearly revealed that deposited gold nanostructures at 5° and 10° of oblique angles are well-separated and tilted in the desired location (Fig. 2a and b). However, we could not observe any individual directional gold nanostructure when the substrate oblique angle ($\alpha$) was at 20° (Fig. 2c). The tilt angles of gold nanostructures were measured from the cross-sectional SEM images using freeware IMAGEJ image analysis software and found to be 38° ± 4° for $\alpha = 5°$ and 62° ± 6° for $\alpha = 10°$, respectively (Fig. S1†). The gold nanorod densities were also calculated as $4.12 \times 10^8$ nanorods $cm^{-2}$ for $\alpha = 5°$ and $5.84 \times 10^8$ nanorod $cm^{-2}$ for $\alpha = 10°$ (Fig. S2–4†). Our result is consistent with the majority of the reports for OAD. Liu *et al.* reported that silver nanorods prepared by OAD fused together and formed a porous network without any directionality at an incident angle larger than 20°, whereas they formed well-separated nanorod array having uni-directionality at an incident angle lower than 20° as similar to our results.[12] However, we should note that this incident angle needed to fabricate low-density directional nanostructures may be varied depending on deposited material and solid substrate due to the self-shadowing effect. In addition to these, we also investigated the X-ray diffraction (XRD) pattern of the deposited AuNRs and found that it reveals strong evidence for the directional growth of AuNRs (Fig. S5†). The strong and sharp peak at $2\theta = 38°$ can be assigned to (111), whereas other diffraction peaks, which are typically due to the face centered cubic crystal system, are diminished attributed to the highly oriented nanoarrays of AuNRs.

Before studying the directional wetting, we have measured the equilibrium water static contact angles for all the fabricated gold nanostructures. Because pure gold is considerably hydrophilic (33.6° ± 2.7°), they were first modified with thiol molecules having different hydrophobic moieties such as –$CF_3$, $CH_3$, and phenyl. These end groups were chosen because of their low surface free energies, and most of the studies about wetting phenomenon have also been reported related to them. For –$CF_3$ modified surfaces, water contact angles were found to be 138.2° ± 4.1 for gold nanofilms prepared at $\alpha = 5°$, 130.6° ± 3.6° for $\alpha = 10°$, 115.4° ± 5.1° for $\alpha = 20°$, and 107.3° ± 3.3° for flat gold film, respectively. Similar tendencies were also observed for both –$CH_3$ and –phenyl modified surfaces as shown in Fig. 3. Pitt *et al.* reported that the surface free energy decreases in the order –phenyl > –$CH_3$ > –$CF_3$.[15] In parallel with their surface free energies, –$CF_3$ modified surfaces, as expected, exhibited better hydrophobicity for all

situations than others. In addition to surface chemistry, the results also clearly revealed that the wetting behavior of the gold nanofilms is highly dependent on the surface morphology caused upon the formation of nanostructures. As mentioned above, the surfaces fabricated at $\alpha = 5^\circ$ have low-density gold nanostructure array. An increment at deposition angle causes an increase in structural density. As a result, the gaps between the nanostructures, which provide the air to be trapped beneath liquid droplets, are reduced and water contact angle values correspondingly decrease.[9] To substantiate our conclusion, the surface roughness values of deposited AuNRs were determined by AFM (Fig S6†). Root mean square (RMS) roughness values were found to be 188.69 nm for $\alpha = 5^\circ$, 98.32 nm for $\alpha = 10^\circ$, and 39.79 nm for $\alpha = 20^\circ$, respectively. It is clear that surface roughness decreased with increasing of the deposition angle.

As mentioned above, the uni-directional wetting behavior using a synthetic engineered nanofilm has been first reported by Demirel and co-workers.[13] In their work, they fabricated directional nanofilms having chlorophenyl end group based on oblique angle polymerization (OAP). The directional wetting of fabricated nanofilms was then quantified by critical droplet volume ($V_c$) which may hold on to the nanofilm surface at an angle. To further understand the directional wetting phenomenon, following a similar approximation, we fabricated our directional gold nanofilms having varying tilt angles and modified with different thiol molecules as mentioned above. For better comparison, the directional wetting was then quantified in the same manner reported by Demirel *et al.*[13] We first evaluated the effect of surface chemistry on the directional wetting. Fig. 4a–c show the critical droplet volumes as a function of the nanofilm tilt angles. We should note that all nanofilms, which were used, were fabricated at the same oblique angle ($\alpha = 5^\circ$). As expected, all the $V_c$ values obtained from anti-parallel axis are larger than their parallel axis values for all tilt angles. Meanwhile, they exhibited observable differences in $V_c$ values depending on their surface chemistries. For directional nanofilms having phenyl end group, the ratio of $V_c$ for anti-parallel axis to $V_c$ for parallel axis ranges from 1.22 ± 0.03 to 1.4 ± 0.08 for tilt angles between 25° and 90°, whereas these ratios range from 1.18 ± 0.02 to 1.36 ± 0.06 for $-CH_3$ modified nanofilms, and 1.15 ± 0.04 to 1.33 ± 0.08 for $-CF_3$ modified nanofilms, respectively. In their work Demirel *et al.* have reported that this ratio ranges from 1.12 to 1.29 for tilt angles between 40° and 80°.[13] It is clear that surface chemistry has an obvious effect on the directional wetting, and such an effect is mainly due to the differences in the surface free energies of chemical end groups onto the nanofilm surfaces. In addition to these, we have calculated the retention forces for modified surfaces, which are needed to start a drop moving on a surface, using eqn (1) proposed by Furmidge.[16]

$$F_{\text{adhesion}} \geq mg \sin a - \gamma_{\text{LVw}}(\cos \theta_{\text{rec}} - \cos \theta_{\text{adv}}) \quad (1)$$

where, $F_{\text{adhesion}}$ is the retention force, $\gamma_{\text{LV}}$, $a$, $m$, and $g$ are also defined to be the surface tension of liquid (in our case water), substrate tilt angle, drop mass and gravity, respectively. Similar to critical droplet volumes, we have found that retention forces were obviously changed depending on the surface chemistries of AuNRs (Fig. S7†). For all cases, forces at antiparallel axis are higher compared to parallel axis.

In order to evaluate the effect of surface morphology, we employed three different nanofilms fabricated by OAD at varying oblique angles ($\alpha = 5^\circ$, 10°, and 20°), and modified them with thiol molecules having phenyl end groups, which exhibit the best directional wetting behavior compared to others. Fig. 4d–f shows the critical droplet volumes for nanofilms fabricated at $\alpha = 5^\circ$, 10°, and 20° as a function of the nanofilm tilt angles. We observed that all the $V_c$ values at anti-parallel directions were decreased with the increase of oblique angles. Increasing the oblique angle to 10° decreases the ratio of $V_c$ for anti-parallel axis to $V_c$ for parallel axis from 1.22 to 1.16. In the case of $\alpha = 20^\circ$, these ratios also ranged from 1.10 to 1.0 for substrate tilt angles between 25° and 90°. As mentioned above, the tilt angles of gold nanostructures ($\beta$) were found to be 38° ± 4° for $\alpha = 5^\circ$, 62° ± 6° for $\alpha = 10^\circ$, and 82° ± 6° for $\alpha = 20^\circ$, respectively (Fig. S1†). The gold nanorod densities were also calculated as $4.12 \times 10^8$ nanorods $cm^{-2}$ for $\alpha = 5^\circ$ and $5.84 \times 10^8$ nanorod $cm^{-2}$ for $\alpha = 10^\circ$. For $\alpha = 20^\circ$, however, we could not calculate the density because there is no individual nanostructure onto the nanofilm surface. To understand the anisotropic wetting phenomenon on our surfaces, we believe that it would be wrong to consider one wetting state (*i.e.*, Wenzel's, Cassie's, Transition or Gecko). Thus, in our opinion, different states should be considered and their contributions should be kept in mind. Various effects such as pinning, contact area, three-phase contact line, van der Walls interactions between drop and substrates, capillary effect and trapped air in the surface nanostructures may play an important role in some degree during the water droplet adhesion. However, among the above mentioned effects, it is believed that the directional wetting is mainly derived from the contact line pinning onto the nanostructures.[6] In the case of parallel axis, the nanostructures onto the nanofilms separate from each other, and therefore they formed a discontinuous three phase contact line (TCL) which provides a small energy barrier to release water droplet deposited on the surface more easily. Meanwhile, there is no enough contact between the droplet and trapped air in the nanostructures.[6] As for antiparallel axis, the nanostructures are closer to each other than parallel direction and form a quasi-continuous TCL which allows the adhering of water droplets to

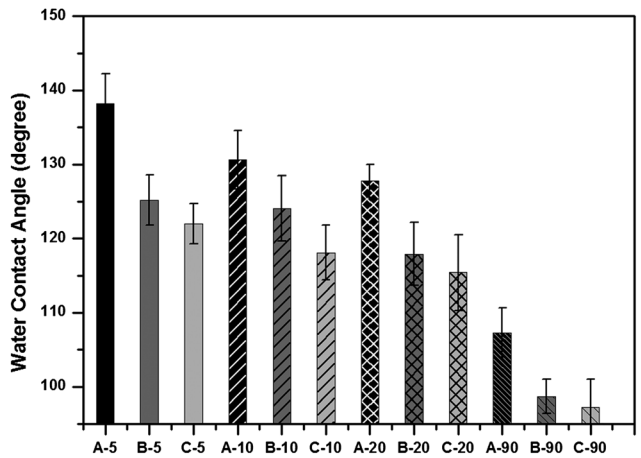


**Fig. 3** Equilibrium water static contact angles for thiol modified gold nanostructures (A = $-CF_3$, B = $-CH_3$, and C = –phenyl). The numbers (5, 10, 20, and 90) in the figure indicate the deposition angles.

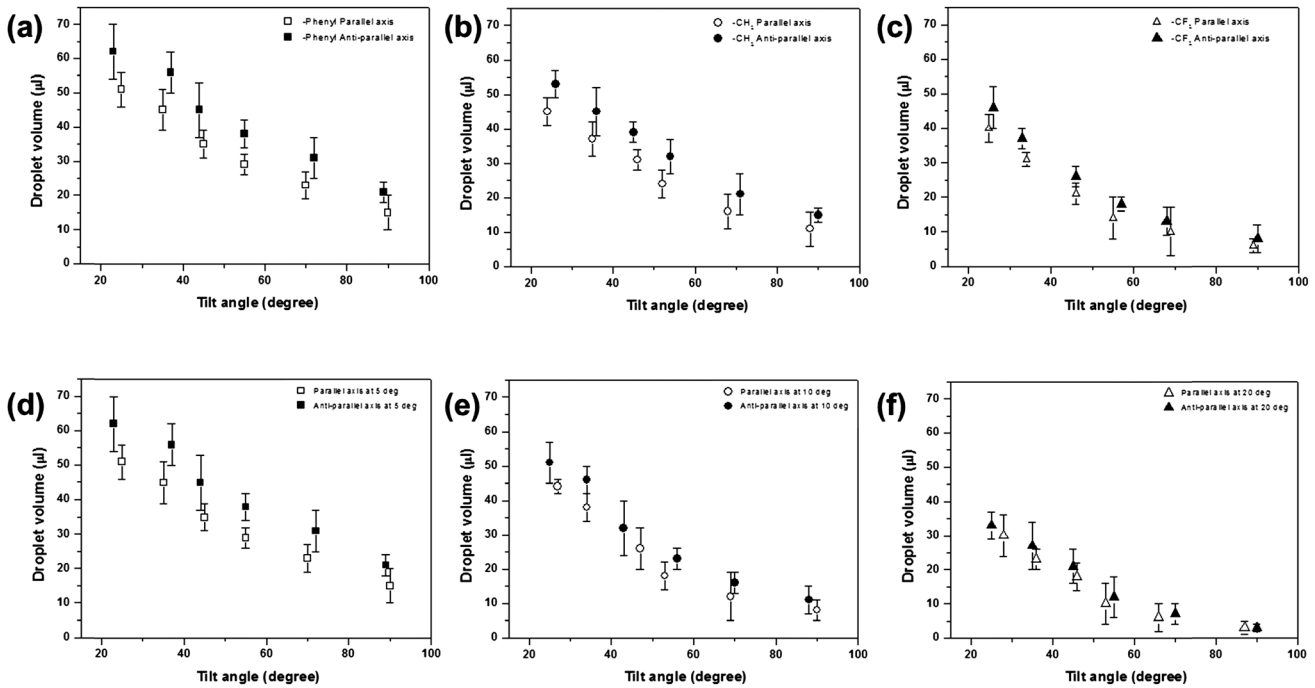


**Fig. 4** (a–c) Critical droplet volumes ($V_c$) as a function of the surface chemistry (a) and morphology (d–f) at different substrate tilt angles.

the surface. Increasing $\beta$ caused to form a denser film and reduce the directionality. Such a transformation can affect the formation of TCL and trapped air between the nanostructures which are responsible for the directional wetting. Meanwhile, our results are somewhat contrary to Demirel's report.[13] In their studies, they proposed based on their theoretical model that increasing the column tilt angle increases the ratio of $V_c$ values. This apparent contradiction may arise from the differences between the mechanisms of OAP and OAD. In OAP, it is difficult to control the nanostructures' tilt angle, length, and their densities onto the surface due to the high affinity of monomer vapor to the surface as well as each other. Contrary to OAP, OAD may allow to control these properties upon deposition parameters. However, the mechanism of directional wetting requires further investigation.

## Conclusions

We have demonstrated the effects of surface chemistry and morphology on the directional wetting phenomenon by using gold nanofilms fabricated using the OAD technique. The gold nanofilms modified with thiol molecules having a phenyl end group exhibited better direction dependent wetting behavior compared to other modified surfaces. Moreover, we found that the critical droplet volumes for both directions were decreased with the increase of nanostructure tilt angle. Obviously, surface chemistry and morphology play a critical role for directional wetting. We believe that our results may contribute to a better understanding and control of directional wetting phenomenon onto the solid surfaces having anisotropic nanostructures. Such a control offers exciting opportunities for several applications involving microfluidic platforms, plasmon-enhanced catalysis, tissue engineering, and biosensors, and we are currently investigating potential uses of our systems in these research areas.

## Acknowledgements

GD and LK gratefully acknowledge the TUBITAK (Project no. 111M237) and Gazi University for financial support (Project no. 05/2012-06). EP was also supported by the Turkish Academy of Science as a full member.

## References

1 L. Kesong, X. Yao and L. Jiang, *Chem. Soc. Rev.*, 2010, **39**, 3240–3255.
2 D. Xia, L. M. Johnson and G. P. Lopez, *Adv. Mater.*, 2012, **24**, 1287–1302.
3 S. Tawfick, M. De Volder, D. Copic, S. J. Park, C. R. Oliver, E. S. Polsen, M. J. Roberts and A. J. Hart, *Adv. Mater*, 2012, **24**, 1628–1674.
4 M. J. Hancock, K. Sekeroglu and M. C. Demirel, *Adv. Funct. Mater.*, 2012, **22**, 223–2234.
5 J. W. M. Bush, D. L. Hu and M. Prakash, *Adv. Insect Physiol.*, 2007, **34**, 117–192.
6 Y. M. Zheng, X. F. Gao and L. Jiang, *Soft Matter*, 2007, **3**, 178–182.
7 G. B. Demirel, F. Buyukserin, M. A. Morris and G. Demirel, *ACS Appl. Mater. Interfaces*, 2012, **4**, 280–285.
8 G. O. Ince, G. Demirel, K. K. Gleason and M. C. Demirel, *Soft Matter*, 2010, **6**, 1635–1639.
9 G. Demirel and U. Tamer, *Nanotechnology*, 2012, **23**, 225604.
10 V. K. S. Hsiao, W. D. Kirkey, F. Chen, A. N. Cartwright, P. N. Prasad and T. J. Bunning, *Adv. Mater.*, 2005, **17**, 2211–2214.
11 G. Demirel, N. Malvadkar and M. C. Demirel, *Thin Solid Films*, 2010, **518**, 4252–4255.
12 Y. J. Liu, H. Y. Chu and Y. P. Zhao, *J. Phys. Chem. C*, 2010, **114**, 8176–8183.
13 N. Malvadkar, M. J. Hancock, K. Sekeroglu, W. J. Dressick and M. C. Demirel, *Nat. Mater.*, 2010, **9**, 1023–1028.
14 S. Neuhaus, N. D. Spencer and C. Padeste, *ACS Appl. Mater. Interfaces*, 2012, **4**, 123–130.
15 A. R. Pitt, S. D. Morley, N. J. Burbidge and E. L. Quickenden, *Colloids Surf., A*, 1996, **114**, 321–335.
16 C. G. L. Furmidge, *J. Colloid Sci.*, 1962, **17**, 309–324.